Inelastic collisions of He^+ and Ar

R. C. Isler
Department of Physics, University of Florida, Gainesville, Florida 32601
(Received 14 January 1974)

Relative emission cross sections have been measured for spectral lines in the vacuum ultraviolet region which are produced by collisions of He^+ with Ar over a range of energies from threshold to 10 keV. The lines investigated arise from the following excited states of Ar and Ar^+: for Ar, $3p^5 4s[^1P, ^3P]$; for Ar^+, $3s3p^6\,^2S$, $3d\,^2P$, $3d\,^2D$, $4s\,^2P$, and $4s'\,^2D$. Charge exchange at low collision energies is dominated by transfer into the $3s3p^6$ states. The cross section for exciting this configuration rises rapidly from threshold at 4.7 eV to a low-energy maximum which occurs at 11.3 eV. By normalizing our data to the absolute emission cross section which has been determined by De Heer *et al.* at a collision energy of 2 keV, it is found that the cross section for exciting the $3s3p^6$ configuration is 5.4×10^{-17} cm^2 at the low-energy maximum. Oscillations are observed in several of the emission cross sections which indicate interferences between the wave functions of one or more of the excited states of the quasimolecule.

I. INTRODUCTION

Several studies of low-energy collisions of the $He^+ + Ar$ complex have been performed both to investigate the potentials of the quasimolecular system and to examine the curve-crossing phenomena which play such an important part in the inelastic processes. Aberth and Lorents have measured the differential elastic scattering,[1] and their results have been analyzed to obtain a diabatic potential curve for the elastic channel.[2] The mechanisms for charge transfer have been studied by Smith, Fleischmann, and Young[3] through observations of the differential scattering of helium atoms at collision energies up to 300 eV. Over 50% of the charge exchange is observed to take place through channels that produce excited states, rather than the ground state, of Ar^+. The reason for such a result is clear from the ordering of the asymptotic energy levels of the diatomic system as shown in Fig. 1 and the realization that the potential curves of the quasimolecule are essentially repulsive. These circumstances imply that the diabatic elastic curve for $He^+ + Ar$ rises steeply and crosses the potential curves which dissociate to $(Ar^+)^* + He$ before it crosses the curve which dissociates to $Ar^+ + He$.[3] Transitions from one state to another most probably take place in the regions of the crossings where they are coupled strongly, so it is not unexpected that a large fraction of the Ar^+ produced by charge transfer is excited. Champion and Doverspike have verified this conclusion by direct observations of the Ar^+ ions that are formed with internal excitations of 11 eV or more.[4] At a collision energy of 94 eV, they find that the cross section for producing these ions in the forward cone out to 60° is 0.9×10^{-16} cm^2, about one-half of the total cross section determined by Koopman[5] for the production of slow Ar^+ ions.

The identification of individual excited states from data obtained through collision spectroscopy is difficult because many of the inelastic channels are quite close in energy. For example, in the work of Ref. 3 it is only possible to identify uniquely the features of the charge-transfer cross section leading to $He + Ar^+(3s3p^6)$ and $He(1s2s) + Ar^+$. Data for the other channels are not resolved.

The determination of populations of the various product states excited by inelastic collisions can often be made through optical spectroscopy, which affords a high degree of resolution. To this end, Lipeles and other workers have studied charge exchange below 1 keV in the $He^+ + Ar$ system by measuring the relative emission cross sections for several Ar II lines which appear in the visible region of the spectrum.[6-8] The observed lines arise from transitions between two excited states, and the strongest of these originate from $4p'$ and $4p$ configurations.[9] Several of these cross sections are not smoothly varying functions of energy but, instead, show highly developed structures which indicate that single isolated curve crossings are not responsible for excitation of the spectral lines and that a more complex theory is necessary to explain the results.

Jaecks *et al.* and De Heer *et al.* have measured emission cross sections for lines in both the visible and the vacuum ultraviolet regions of the spectrum at collision energies from 0.3 to 10 keV.[10,11] Their results reveal the general features of the emission cross sections in this region, but the data are taken at increments too large to reveal whether any detailed structures such as those

observed by Lipeles are also present in the region of large impact energies.

In the present work, the emission cross sections for the lines in the vacuum ultraviolet region which originate from the lowest excited states of Ar and Ar^+ have been investigated from threshold to 10 keV. It is the effects of these low states which appear predominantly in the inelastic differential scattering at energies below 300 eV, but no optical studies that can be correlated with these direct measurements have heretofore been performed. The energy range above 300 eV has been examined in more detail than in the investigations of De Heer *et al.* in order to see if any additional features are apparent that are not revealed in their studies.

II. EXPERIMENTAL APPARATUS AND TECHNIQUE

The apparatus used in the present experiments is described in detail elsewhere.[12,13] Briefly, it consists of an electron-bombardment ion source, a buffer chamber which incorporates a set of electrostatic lenses and a low-resolution Wien filter, and a collision chamber which contains the target gas. Typical ion currents vary from 2×10^{-8} A at 10 eV to 5×10^{-6} A at energies above 1 keV. The beam is refocused at each energy to obtain the maximum current into the collision chamber. A pair of simple retarding grids has been used to measure the spread in the energy of the beam, and the full width of the distribution at half-maximum intensity appears to be 3.6 eV. There are indications from some measurements on the $He^+ + Ne$ system that the spread in beam energy is actually smaller than 3.6 eV because oscillatory features of the excitation cross sections which are separated by 5 eV appear to be resolved better than would be possible with a beam that has such a broad distribution. Also, the mean energy of the ions is 12.3 ± 0.5 eV lower than the potential applied to the ion chamber, and this correction has been applied in plotting the curves for emission cross sections shown in Figs. 3–9.

The first several excited states of Ar^+ make transitions only to the ground state, and the spectral lines appear in the vacuum ultraviolet region below 1000 Å. Lines of interest are selected by using a McPherson model 225 normal-incidence vacuum monochromator, and are detected with a Bendix model 306 particle detector that has a tungsten cathode. Emission cross sections for the resonance lines of Ar I at 1048 and 1067 Å have also been measured, but without using the monochromator for spectral resolution. Instead, the detector is coupled directly to the collision chamber with a 1-mm LiF window in front of the cathode. This combination of window and detector is sensitive only to radiation between about 1050 and 1250 Å. Spectral scans show that other than the resonance lines of the atom, only the Lyman-α line is detectable in this region. The intensity of this impurity line is independent of the target-gas pressure and most likely arises from collisions of He^+ with residual hydrocarbons. The contribution of the Lyman-α line [(5–10)%] to the signal is obtained by recording the counts at each energy investigated without gas in the target chamber. These counts are then subtracted from the total number obtained with the target gas in the chamber in order to obtain the emission cross section for the resonance lines.

Emission cross sections appear to be constant as a function of pressure of the target gas up to 2.5×10^{-4} Torr. It is found, however, that relative cross sections can be obtained with pressures as high as 10^{-3} Torr. An example of data taken at these two pressures is shown in Fig. 3, in which duplicate measurements of the cross section for exciting the $3s3p^6$ state of Ar^+ are shown for energies below 20 eV. The crosses are from data taken at 10^{-3} Torr and the dots are from data taken at 2.5×10^{-4} Torr. The two sets of points have been adjusted for the best least-squares fit. The shapes of the two curves are seen to be in good agreement down to 10 eV; below this energy they appear to be shifted by 1 eV or less. As noted previously, there is an uncertainty of

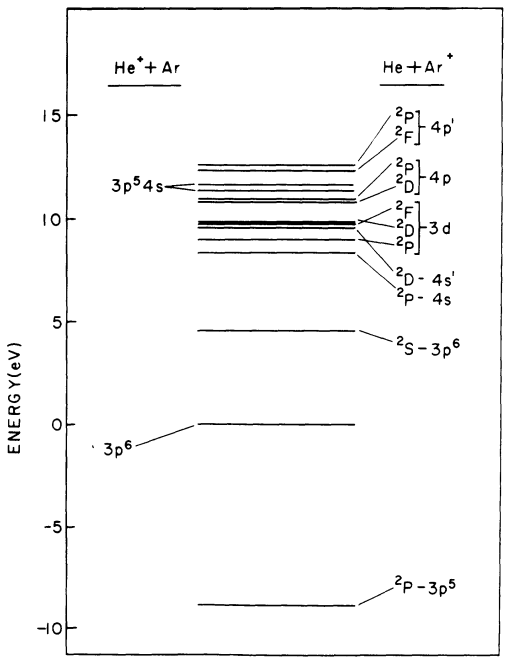

FIG. 1. Energy levels of the $(He+Ar)^+$ system.

±0.5 eV in the mean energy of the ions, and the discrepancies between the two curves are undoubtedly caused by this inaccuracy rather than by the difference in pressure. Data taken at higher energies—up to 1 keV, where an uncertainty of ±0.5 eV is not significant—showed agreement for the two target pressures within the statistical uncertainties.

The counting periods for each collision energy are 100 sec or more for lines which are selected by the monochromator. At least three separate sessions of recording data are required to obtain the emission cross section for a single line over the entire energy range from threshold to 10 keV. The data taken at different times are fitted by computing cross sections for several identical energies during successive sessions and then adjusting all the points with a normalization constant that is obtained from the best least-squares fit at these selected energies.

III. RESULTS

Spectral scans of the region from 550 to 1100 Å are shown in Fig. 2. These scans have been obtained at collision energies of 300, 65, and 23 eV. Many of the strong transitions are grouped between 650 and 750 Å and are not resolved in Fig. 2. These results support the conclusions reached by Smith, Fleischmann, and Young that excitation to the $3s3p^6$ configuration dominates all other inelastic processes at very low energies, but that excitation to several other configurations is highly probable at collision energies of 65 eV or more.

The most intense features other than the doublet at 920 and 932 Å arise from the following states of the argon ion: $4s\,^2P$, $4s'\,^2D$, and $3d^2D$. Several other weaker groups of lines are also seen, including the 1048- and 1067-Å resonance lines of ArI. It is not possible to determine if the line at 584 Å originates from the $3d'\,^2D$ state of Ar^+ or from the $2\,^1P$ state of He; it is most likely a blend of the two transitions. De Heer *et al.*[11] assume that this line originates from $Ar^+(3d'\,^2D)$, and, indeed, other lines from this state are apparent near 584 Å. However, Isler and Nathan[14] have shown that charge exchange into excited states of neutral helium does occur, and Smith, Fleischmann, and Young[3] could readily detect the production of metastable helium in their work. As noted in previous spectral investigations, ex-

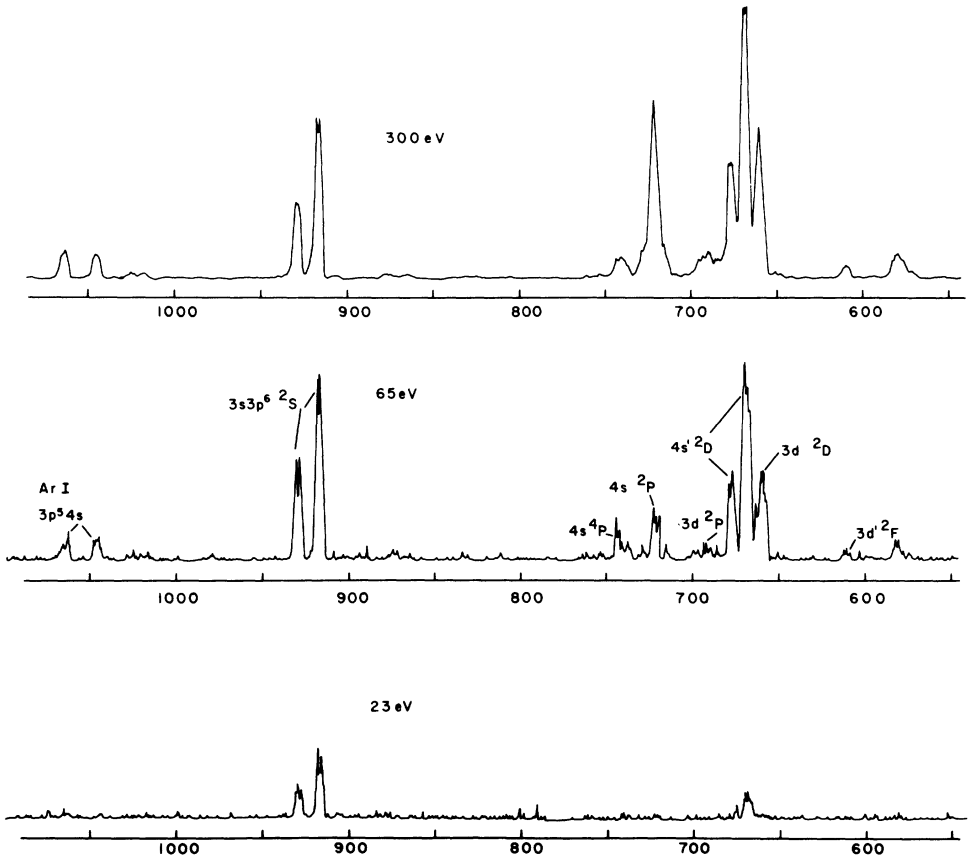

FIG. 2. Far ultraviolet spectra produced by $He^+ + Ar$ collisions at 300, 65, and 23 eV.

TABLE I. Spectral lines observed in He^+ +Ar collisions. The absolute emission cross sections and cascade contributions are those measured by De Heer *et al.* (Ref. 11) at a collision energy of 2 keV.

Ion	Wavelength (Å)	Upper state	Cross section (10^{-17} cm^2)	Cascade cross section (10^{-17} cm^2)
Ar^+	920 932	$3s3p^6\,^2S$	5.42	small
	718 723 726 731	$4s\,^2P$	0.77	0.74
	691 693 698	$3d\,^2P$	0.81	unknown
	679	$4s'\,^2D$	2.02	0.67
	662	$3d\,^2D$	5.11	small
Ar	1048 1067	$4s[^1P, ^3P]$	0.470	unknown

citation to quartet states is generally far less probable than excitation to the doublet states; however, a group of lines which arise from the $4s\,^4P$ state is seen in Fig. 2 and is as prominent as the emission from the $4s\,^2P$ state at a collision energy of 65 eV.

The relative emission cross sections were obtained for the most prominent lines or groups of lines; the wavelengths are listed in Table I. The response of our optical system has not been measured, but absolute cross sections can be established by normalizing our data at 2 keV to the values that are stated in Ref. 11. These values, together with estimates of the cascade contributions, are also listed in Table I. The cross section for the weak lines originating on the $3d\,^2P$ state was estimated from the scan of Fig. 2 by comparing the intensity of these lines to the stronger features on either side of them and utilizing a linear interpolation. There is no evaluation of the contributions of cascades in populating the $3d\,^2P$ state.

The close spacing of the spectral lines in the 650- to 750-Å region requires the use of narrow monochromator slits to obtain resolution, thereby decreasing the counting rate. Complete isolation of single spectral lines or a group of lines with a common upper term is not feasible in many cases because the counting rate becomes too small for obtaining adequate statistics in a reasonable time. Those groups which originate from the $4s'\,^2D$ and $3d\,^2P$ terms have been taken with bandwidths which encompass some very weak transitions from quartet levels. Spectra taken at higher resolution than those of Fig. 2 indicate that these intercombination lines should comprise less than 5% of the measured intensity within the passband of the monochromator. Also, the line at 662 Å ($3d\,^2D$) could not be completely isolated from the one at 666 Å ($3d\,^2F$), and the latter makes a contribution of about 8% to the cross section that is attributed to the $3d\,^2D$ state.

The emission cross sections of the various lines observed are shown in Figs. 3–9. The statistical uncertainty in each point is less than 5% except at the lowest energies, where the curves decline as threshold is approached. The vertical scale gives relative measurements only for a particular curve. The scales for the cross sections have been chosen to give a very rough idea of the relative intensities of the various lines as detected without correcting for the variable transmission of the monochromator or the sensitivity of the

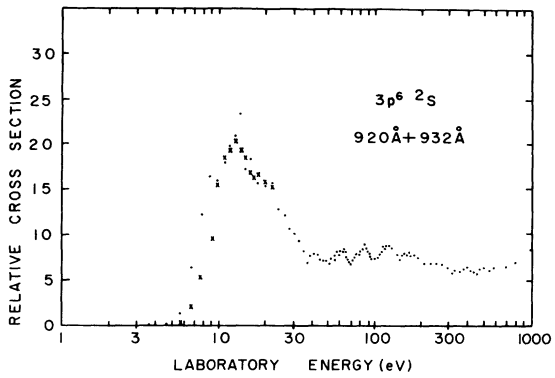

FIG. 3. Emission cross section below 1 keV for the $3s3p^6\,^2S$ state of Ar^+.

detector. At energies above 300 eV our relative cross sections are similar to those obtained by De Heer *et al.*, although some minor fluctuations, notably in Fig. 5 for the $3d\,^2D$ state, can be seen. Below 300 eV most of the cross sections have a complicated oscillatory structure.

IV. DISCUSSION

One of the most striking features of $He^+ + Ar$ inelastic collisions revealed by Figs. 3–9 is the dominance of excitation to the $3s3p^6\,^2S$ state at low energies. The cascade contribution to the emission cross section is negligible, and the curve of Fig. 3 is essentially that for the primary excitation process, at least at low energies. The rapid rise of the emission cross section just above threshold indicates that excitation into this state is highly probable at collision energies which are below the thresholds for exciting any others; by normalizing our data to the absolute cross sections determined by De Heer *et al.* at 2 keV, it is found that this cross section has a value of 4.1×10^{-17} cm^2 at the collision energy which is required to excite the next lowest state, 9.32 eV (in the laboratory system). Also, even though the final state $Ar^+(3s^23p^5) + He(1s^2)$ is produced as an exothermic product, its threshold is above 20 eV.[3] Most of the charge exchange which takes place in low-energy gas discharges of helium and argon undoubtedly takes place through the $3s3p^6\,^2S$ state. Such charge-exchange processes which lead to population inversions might ultimately be exploited to produce lasers which operate at wavelengths in the vacuum ultraviolet region of the spectrum.

Much of the analysis by Smith, Fleischmann, and Young for the collisional spectroscopy of the $(He + Ar)^+$ system relates to the scattering from the $3s3p^6\,^2S$ state because the features of this process are well isolated in the data from those of other channels. It is possible to correlate some of the present work with these results. First, the threshold taken from the average of the two sets of our low-energy data is 4.7 ± 0.5 eV in the center-of-mass system; the error reflects the uncertainty in the mean energy of the ion beam as noted in Sec. II. This value lies above the threshold of 4.3 eV deduced from the work of Ref. 3. However, thresholds for the production of atomic lines are not the same as those deduced from measurements of the differential scattering if the curve crossing occurs within a potential well of the upper state. In order for the two particles to separate and subsequently produce radiation, the collision energy must be greater than the asymptotic difference of the initial and final states. For the $3s3p^6\,^2S$ state this difference is 4.66 eV, so that the experimental result shows only that the crossing occurs at a point on the upper curve where the contribution of the polarization term to the potential is greater than or equal to that of the Coulomb repulsion.

A second point of comparison with Ref. 3 lies in the establishment of the location of the low-energy maximum for the excitation to the $3s3p^6\,^2S$ state. In the previous work this maximum was not measured directly because the detection of unexcited neutral particles at low energies is not feasible; instead, the elastic perturbation was used to determine that the peak was at 36 eV. It is seen from Fig. 3, however, that the low-energy maximum occurs at 11.3 eV in the center-of-mass system. This difference lowers the estimate of the upper bound of the matrix element which couples the two channels in the Landau-Zener model. In this model, the probability that a transition takes place from the incoming channel B to the excited state C in the region of a potential crossing is

$$P = 2\exp(-v_{LZ}/v_{r,l})[1 - \exp(-v_{LZ}/v_{r,l})], \tag{1}$$

where $v_{r,l}$ is the radial velocity at the crossing for a particle which has an angular momentum $[l(l+1)]^{1/2}\hbar$. The parameter v_{LZ} is given by

$$v_{LZ} = 2\pi(H_{BC})^2/\hbar|\Delta V'_{BC}|\,, \tag{2}$$

in which H_{BC} is the matrix element which couples channel B to channel C, and $\Delta V'_{BC}$ is the difference in slopes of the two potentials which can be obtained from the parametrized curves of Ref. 3. Both quantities are evaluated at the crossing point. The radial velocity at which the maximum in the cross section occurs is related to v_{LZ} by

$$v_{LZ} = (\ln 2)v_{max}\,, \tag{3}$$

and the relative velocity of the two particles at the crossing point is

$$v_{r,l} = \left[\frac{2}{\mu}\left(E_{c.m.} - V(R) - \frac{l(l+1)\hbar^2}{2\mu R^2}\right)\right]^{1/2}, \tag{4}$$

where R is the distance at which the crossing occurs. By setting $l = 0$ we obtain the maximum possible radial velocity at a given collision energy. With a value of 11.3 eV for $E_{c.m.}$, it is found that

$$H_{BC}(R) \leq 0.38 \text{ eV}\,, \tag{5}$$

instead of 0.55 eV as obtained by using $E_{c.m.} = 36$ eV.

Rather than obtaining just an upper bound for H_{BC}, one may sum over all impact parameters and fit the resultant to the experimental data. The excitation cross section is given by

$$Q = \frac{2\pi}{k_0^2}\sum_l (2l+1)P(v_{r,l})\sin^2\tau_l\,, \tag{6}$$

where τ_l is a phase factor which gives rise to oscillations in the differential cross sections (but not in the total cross sections).[15]

This phase factor is computed from the difference in wave number which develops between the two possible trajectories that a system can take after passage through the crossing point. Its calculation requires a numerical integration for each value of l. In order to obtain some estimate of H_{BC} without having to perform the integrations, we assume that even though the factors $\sin^2\tau_l$ modulate the differential cross section for fixed energy, their effect on the total cross section is about the same at all energies. Therefore we set τ_l equal to a constant and perform the sum indicated by Eq. (6). The total cross section Q computed using this approximation decreases much too slowly at energies above the maximum to obtain a good fit to the data of Fig. 3 below 100 eV. However, an estimate of H_{BC} may be obtained by calculating the value of v_{LZ} that brings the measured and computed peaks into alignment. This value is

$$v_{LZ} = 0.15 \times 10^6 \text{ cm/sec}, \tag{7}$$

and the coupling parameter calculated from Eq. (2) is

$$H_{BC} = 0.12 \text{ eV}. \tag{8}$$

The use of the Landau-Zener approximation for analyzing the present data is, of course, questionable. Several assumptions and limitations of this formalism have been discussed in the literature.[16] In addition, a two-state approximation, even for pairs of states which are well separated in energy from any others, may not be at all correct. Numerical solutions of several coupled scattering equations[15] may be required in all but the simplest cases in order to characterize the collision process with reasonable accuracy.

Besides the low-energy maximum, other prominent features of Fig. 3 are the oscillations in the region from 35 to 500 eV. These variations in the total cross section arise from an interference in the wave functions of two excited channels at some distance R_0, outside the primary crossings. The phase difference of the two functions, which develops upon separation of the particles, is given by

$$\varphi_{DC} = \int_{r_D}^{R_0} K_D(r)\,dr - \int_{r_C}^{R_0} K_C(r)\,dr + \phi_0 \tag{9}$$

(see Ref. 17). The integrations are taken from the primary crossing points to R_0, and the wave numbers $K(r)$ are calculated from Eq. (4) and the relationship

$$K(r) = \mu v_r/\hbar\,(v_r/\hbar). \tag{10}$$

It has been shown that φ_{DC} is essentially independent of impact parameter for large values of l, and therefore oscillations appear in the total cross section.[18] If R_0 is much greater than the impact parameter and if the kinetic energy of the colliding particles is much greater than the potential difference from the turning points to R_0, then Eq. (9) can be written as

TABLE II. Laboratory energies at which the maxima and minima of oscillations occur in the emission cross sections. Values of Γ are calculated from successive maxima.

State	E_{max} (eV)	E_{min} (eV)	$1/v$ (10^{-6} sec/cm)	$1/v' - 1/v''$ (10^{-6} sec/cm)	Γ (eV Å)
Ar^+					
$3s3p^6\,^2S$	40	36	0.245		
	59	50	0.197	0.048	8.62
	85	69	0.162	0.035	11.82
	119	95	0.135	0.027	15.32
	161	142	0.116	0.019	21.77
	255	208	0.091	0.023	17.99
	385	300	0.074	0.017	24.34
$3d\,^2D$	40	43	0.268		
	52	60	0.225	0.043	9.62
	69	90	0.190	0.035	11.82
	95	(est.)	0.158	0.032	12.93
	138	155	0.128	0.030	13.79
	240	310	0.095	0.033	12.54
	450	600	0.069	0.026	15.91
	750		0.054	0.015	27.58
$4s'\,^2D$	80	93	0.173	0.028	14.77
	110	125	0.145	0.024	17.24
	152	190	0.121	0.021	19.70
	220	270	0.100		
Ar					
$3p^5 4s$					
$[^1P, ^3P]$	34	37	0.314		
	52	69	0.231	0.083	4.98
	94	125	0.160	0.071	5.83
	178	250	0.112	0.048	8.62
	510	1000	0.065	0.047	8.80
	2200		0.030	0.035	11.82

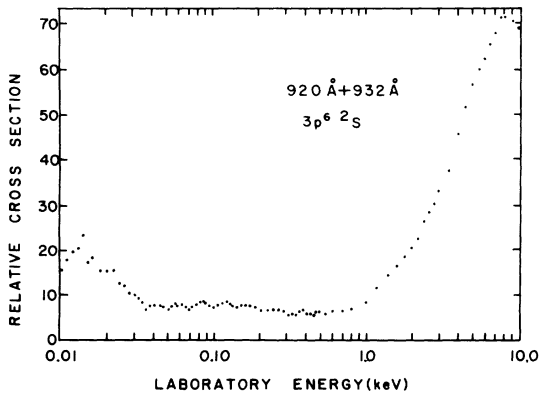

FIG. 4. Emission cross section from 0.10 to 10.0 keV for the $3s3p^6\,^2S$ state of Ar^+.

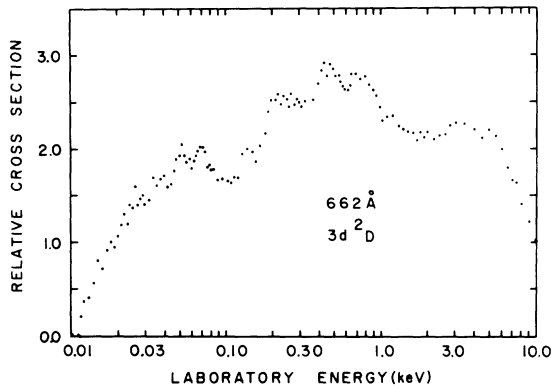

FIG. 5. Emission cross section for the $3d\,^2D$ state of Ar^+.

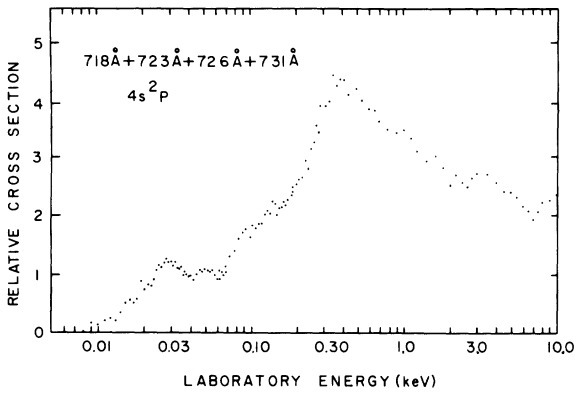

FIG. 7. Emission cross section for the $4s\,^2P$ state of Ar^+.

$$\varphi_{DC} \approx \frac{1}{\hbar v}\left(\int_{r_D}^{R_0} V_D(r)\,dr - \int_{r_C}^{R_0} V_C(r)\,dr\right) + \varphi_0$$

$$= \frac{\Gamma}{\hbar v} + \varphi_0 . \qquad (11)$$

Here, v is the average velocity of separation in the interfering channels and φ_0 is the initial phase difference between the two wave functions. If the conditions exist for Eq. (11) to be valid, then the peaks in the oscillations should be spaced equally as a function of $1/v$, or we can write

$$\Gamma = \frac{2\pi\hbar}{1/v' - 1/v''} , \qquad (12)$$

where v' and v'' are the velocities at two adjacent peaks, and Γ should be constant for any pair of these. Several examples exist in which the phase difference appears to develop as a linear function of $1/v$.[19] This situation does not hold for the emission cross section shown in Fig. 3, as can be seen from the values of Γ listed in Table II. The differences are smaller for the peaks that appear at low energies than they are for the ones that appear at high energies, indicating that the phase development is not completely independent of the impact parameter or that the interference arises from the coupling of more than two states.

In Fig. 4 it is seen that the emission cross section for the $3s3p^6\,^2S$ state rises steeply at energies above 1 keV until it reaches a peak at about 8 keV. De Heer *et al.* have noted that this behavior is consistent with the adiabatic hypothesis as applied to the asymptotic potentials and implies that excitation in this region is not taking place through a localized curve crossing.

Figures 5–8 show the emission cross sections for several states of Ar^+ that are formed by promoting a $3p$ electron to a $3d$ or $4s$ orbital. Determinations of the thresholds for exciting these states are much more uncertain than for the $3s3p^6\,^2S$ state. The signal-to-noise ratios are poor at the low energies, and the slopes of the curves are not steep. The apparent thresholds are listed in Table III together with the minimum energy required for excitation. The threshold for the $4s\,^2P$ state is too low, about 1 eV below the

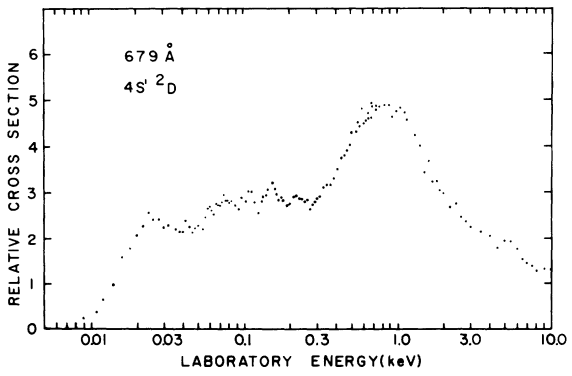

FIG. 6. Emission cross section for the $4s'\,^2D$ state of Ar^+.

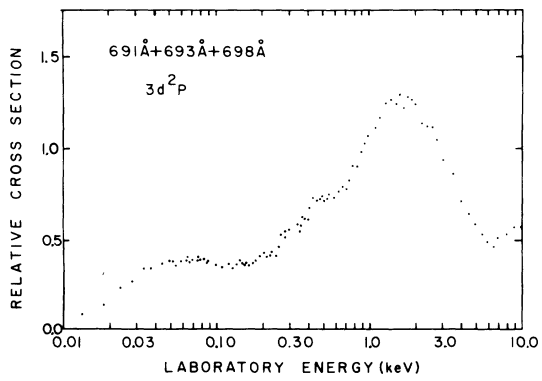

FIG. 8. Emission cross section for the $3d\,^2P$ state of Ar^+.

TABLE III. Thresholds for emission cross sections.

State	Minimum energy for excitation (eV)	Observed threshold (eV)
$3p^6\,^2S$	4.66	4.70
$4s\,^2P$	8.31	7.20
$4s'\,^2D$	9.61	9.50
$3d\,^2D$	9.86	10.08

minimum; the other three are close to the minimum energy required for excitation. Even though it is not possible to pinpoint the thresholds accurately, the experimental results show that the signal-to-noise ratio is at least 1:1 for energies that are 2 eV above the values shown in Table III. This fact indicates that the thresholds are no more than 2 eV above their asymptotic limits and that the potential curves for the excited channels are not strongly repulsive in the region of the crossing.

The emission cross sections for these states have a rather complicated behavior. Excitation at the lower end of the energy range most likely occurs as a result of the elastic-potential curve crossing the various Σ channels which lead to excited final states of Ar^+. The onset of a second excitation process appears to occur in the middle of the energy range, however, and the emission cross sections rise to a maximum and then decrease as the collision energy increases to 10 keV. This second excitation process is not due to the adiabatic criterion being satisfied for the asymptotic states; it occurs at energies which are too low. One possible explanation for the second process is that it is due to the excitation of the Π states by rotational coupling with the incoming Σ channel. Another plausible explanation is that in the intermediate energy range, curve crossings which occur at small internuclear separations provide additional modes for populating excited levels of the argon ion. The excitation may take place either by dissociation from channels which correlate directly to the upper levels of the multiplet under observation, or by secondary crossings which occur between excited channels as the particles separate.

Rapid oscillations are also seen to occur in the cross sections shown in Figs. 5–8. The observed maxima and minima of the oscillations in the low-energy range are shown in Table II, with the values of Γ calculated from the separation of successive peaks. If only pairs of excited states are coupled, the maxima of one should occur at the same energy as the minima of the other. This behavior does appear to hold closely for the first five oscillations of the $3s3p^6\,^2S$ state and the $3d\,^2D$ state, but it is not satisfied at the higher energies. There is no obvious correlation of phases between any other pairs of states. However, in rapidly rising or declining portions of the cross-section curves, the minor fluctuations tend to be obscured, and it is possible that oscillations exist in the $4s\,^2P$ curve which are related in a simple manner to those seen in one of the others. Also, the states which were studied by Lipeles may be coupled to the ones which have been investigated here, but his data have not been recorded at energy intervals spaced closely enough to observe rapid oscillations.

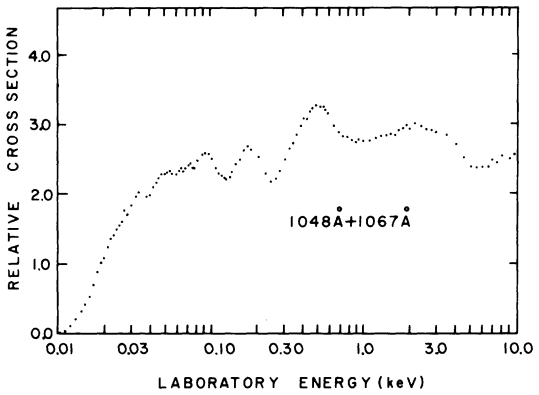

FIG. 9. Emission cross section for the $3p^6 4s[^1P, ^3P]$ states of Ar.

Direct excitation of the argon target is revealed in Fig. 9 by the emission cross section for the resonance lines. Again several oscillations are seen superimposed upon the main curve, which seems to be almost flat above 100 eV. The counting statistics for this data are better than for any other groups of lines observed because the detector arrangement does not require the use of the monochromator. However, the presence of the background signal makes the determination of the threshold even more uncertain than it is for the ionic lines, and a value has not been listed.

Altogether, the results presented here show that the emission cross sections for even the lowest excited states of the $(He + Ar)^+$ system are complex. Both primary and secondary excitation processes seem to take place, and none of the cross sections fall off strictly as E^{-1} up to energies of 10 keV. It is obvious that fairly extensive analysis will be required to explain the details of the excitation processes.

[1]W. Aberth and D. C. Lorents, Phys. Rev. 144, 109 (1966).
[2]F. T. Smith, R. P. Marchi, W. Aberth, D. C. Lorents, and O. Heinz, Phys. Rev. 161, 31 (1967).
[3]F. T. Smith, H. H. Fleischmann, and R. A. Young, Phys. Rev. A 2, 379 (1970).
[4]R. L. Champion and L. D. Doverspike, J. Phys. B 2, 1353 (1969).
[5]D. W. Koopman, Phys. Rev. 154, 79 (1967).
[6]M. Lipeles, Phys. Rev. A 4, 140 (1971).
[7]M. Lipeles, R. D. Swift, M. S. Longmire, and M. P. Weinreb, Phys. Rev. Lett. 24, 799 (1970).
[8]H. Schlumbohm, Z. Naturforsch. 239, 970 (1968).
[9]Unprimed configurations signify that the parent state is ^3P, primed configurations signify that it is ^1D.
[10]D. Jaecks, F. J. De Heer, and A. Salop, Physica (Utr.) 36, 606 (1967).
[11]F. J. De Heer, B. F. J. Luyken, D. Jaecks, and L. W. Muller, Physica (Utr.) 41, 588 (1969).
[12]R. C. Isler, Rev. Sci. Instrum. 45, 308 (1974).
[13]R. C. Isler, Phys. Rev. A 9, 1865 (1974).
[14]R. C. Isler and R. D. Nathan, Phys. Rev. Lett. 25, 3 (1970).
[15]N. F. Mott and H. S. W. Massey, *The Theory of Atomic Collisions*, 3rd ed. (Oxford University, London, 1965), Chap. XIII.
[16]D. R. Bates, in *Atomic and Molecular Processes*, edited by D. R. Bates (Academic, New York, 1962), p. 608; V. K. Bykhovskii, E. E. Nikitin, and M. Ya. Ovchinikova, Zh. Eksp. Teor. Fiz. 47, 750 (1964) [Sov. Phys.—JETP 20, 500 (1965)]; J. B. Delos and W. R. Thorson, Phys. Rev. A 6, 728 (1972).
[17]H. Rosenthal and H. M. Foley, Phys. Rev. Lett. 23, 1480 (1969).
[18]H. Rosenthal, Phys. Rev. A 1, 1030 (1971); V. A. Ankvdinov, S. V. Bobashev, and V. I. Perel, Zh. Eksp. Teor. Fiz. 60, 906 (1971) [Sov. Phys.—JETP 33, 490 (1971)].
[19]S. Dworetsky, R. Novick, W. Smith, and N. Tolk, Phys. Rev. Lett. 18, 939 (1967); N. H. Tolk, C. W. White, S. H. Dworetsky, and L. A. Farrow, Phys. Rev. Lett. 25, 1251 (1970).